Jordan Journal of Civil Engineering, Volume **7**, No. **2**, **2013**

Energy Losses and Turbulence Characteristics through Hydraulic Structures Using Laser Doppler Velocimetry (LDV)

Mahmoud I. Elshewey

Associate Profesor, Water and Water Structures Engg. Dept., Faculty of Engg., Zagazig University, Zagazig, Egypt. E-Mail: m.elshewey@yahoo.com

ABSTRACT

This paper deals with the experimental investigation of energy losses and turbulence characteristics through hydraulic structures in a rectangular channel using Laser Doppler Velocimetry (LDV). Measurements include turbulence intensity components and mean velocity components. Experiments were conducted with different contraction ratios at different expansion angles for different bed slopes. The results show that the rate of variation of the energy loss increases till an expansion angle of about 30°. This rate of increase decreases above this value of expansion angle. The energy loss is quite high at a contraction ratio of 0.7. Also, the results clearly show that gradual expansion decreases the turbulence intensities in the wall and free surface regions compared to sudden expansion. The maximum values of turbulence intensities occur either close to the bed or at the free surface, with minimum values occurring within the core region. The turbulence intensities, however, increase sharply at the free surface due to free surface wave effect, and have the largest value in sudden expansion.

KEYWORDS: Energy losses, Turbulence characteristics, Hydraulic structures, Laser doppler velocimetry, Contraction ratio, Free surface, Froude number, Expansion angle.

INTRODUCTION

The information regarding the turbulence characteristics in transitional structures is somewhat scanty. Paradoxically enough, the problem of separation of the main stream of flow at open channel transitions or at an abrupt change of the boundary attracted the attention of investigators since the earliest time and yet it remains one of the least understood and the most critical problems of fluid dynamics today. Open channel transitions are commonly used in hydraulic structures in a variety of situation to serve as a link with minimum possible energy loss. Open channel transitions have been extensively studied because of their use in water resources engineering and their efficacy in reducing the energy loss in hydraulic structures. Transitions are provided, whenever the size or the shape of the cross-section of an open channel changes. Such changes are often required in natural and artificial channels for water structures for economic as well as for practical reasons. The transitions may be vertical or horizontal, contracting or expanding, sudden or gradual, required for subcritical or supercritical flows. The change in the cross-section disturbs the flow in the contracted reach and near it from both upstream and downstream reaches. The change in the cross-section, slope and/or alignment over a specified reach is termed local transition, such channel transition is used mainly to avoid or minimize excessive energy loss, to eliminate cross waves and the resulting turbulence and to ensure safety of both the structure and the downstream channel reach. In the design of

Accepted for Publication on 12/1/2013.

hydraulic structures, designers do their best to avoid sudden transition of the flow by sudden contractions to ensure smooth flow with minimum energy loss and to reduce the turbulence pattern. As the flow passes through a bridge, a channel transition in the form of contraction and subsequent expansion is involved. Since these transitions are meant for continuous use, their role in the minimization of energy loss and attenuation of turbulence assumes significance. It is indispensable in hydraulic engineering to investigate structures of turbulence behind multi-vent water structures in the expansion zone in order to control turbulent flows and to design hydraulic structures properly. In designing channel transitions, it is necessary to avoid excessive energy loss, to eliminate cross waves and turbulence, to ensure smooth streamlined flow, to minimize standing waves and to prevent the transition from acting as a choke influencing upstream flow. Free surface has a unique role in governing the turbulence in open channel flows. The phenomenon is usually so complicated that the resulting flow pattern is not readily subjected to any analytical solution. So, a practical solution is possible, however, through experimental investigation. The turbulent flow models in open channel flows were discussed by Garde (1993, 1994), Rodi (1993) and Nezu and Nakagawa (1993). Measurements of turbulence characteristics in open channel flows using LDA have been carried out by several investigators (Guoren and Xiaonan, 1992; Nezu and Rodi, 1986; Song and Chinew, 2001; Sukhodolov and Thiele, 1998). Experimental investigations of turbulent structure of back facing step have been reported by several investigators (Amino and Goel, 1985; Nakagawa and Nezu, 1995; Nakagawa and Nezu, 1987; Etheridge and Kemp, 1978). The main results of Formica were reported in Chow (1959). The present study of characteristics and turbulence structure behind multi-vent water structures is a typical case of separation at an abrupt change of boundary. Thus, one of the purposes of studying the turbulence behind water structures in the expansion zone is to gain insight into the properties and interactions of these turbulent structures. Much less information is available regarding the turbulence characteristics in the expansion zone of water structures.

Therefore, precise and accurate measurements of energy loss are carried out to study the variation of energy loss upstream, within and downstream of multi-vent water structures. Also, the present research involves measurements of mean and fluctuating flow characteristics such as streamwise and vertical turbulence intensities and streamwise and vertical mean velocity components in the expansion zone behind multi-vent water structures. The measurements are carried out using Laser Doppler Velocimetry (LDV); a non-intrusive fiber optic state of the art technique, in the expansion zones of water structures at different contraction ratios b/B of 0.9, 0.8, 0.7, 0.6, 0.5 and 0.4 at different expansion angles Θ of 15°, 30°, 45°, 60°, 75° and 90° for various bottom slopes S_o of 0.005, 0.01, 0.015, 0.02 and 0.025. Also, the objectives of the present research are: to use LDV, which includes the data acquisition system data processing to measure mean and fluctuating flow characteristics at different locations in the expansion zones of water structures; to conduct a comparative study of the depthwise variation of streamwise and vertical turbulence intensities at different cross-sections in the expansion zones of water structures; to make a comparative study of the depthwise variation of water structures; to make a comparative study of the depthwise variation of streamwise and vertical mean velocity components. Similarly, the measurements were made in the expansion zones along the centerline at a relative depth ratio y/y_o of 0.5 to study the variation of mean and fluctuating flow characteristics.

THEORETICAL STUDY

In the flow over the water structure through a channel, part of the pressure head will be lost partly due to dissipation of energy in separation zones and partly due to friction between fluid and the channel

wetted parameter. On the other hand, the construction of flow by contraction will result in a corresponding backwater build-up. Figure 3 shows a definition sketch of flow through contraction in a sloping channel. The variables affecting the flow through the multi-vent water structure are shown in the figure and explained at the notation section. The functional relationship of energy loss through the water structure could be written as follows:

$$f_1(g, V_u, Y_u, b, B, Y_d, V_d, \Delta E, \Delta E_u, \Delta E_d, S_o, \Theta) = 0 \quad (1)$$

Using dimensional analysis, the following dimensionless relationship is obtained:

$$\frac{\Delta E}{Y_u} = f_2\left[F_u, \frac{b}{Y_u}, \frac{B}{Y_u}, S_o, \Theta\right]. \quad (2)$$

Keeping in mind the properties on the non-dimensional quantities, the following expression could be obtained from Eq. (2):

$$\frac{\Delta E}{Y_u} = f_3\left[F_u, \frac{b}{B}, S_o, \Theta\right]. \quad (3)$$

It may appear better to analyze energy loss through the water structures as a ratio related to the upstream energy, E_u. Therefore, E_u is used instead of Y_u in the left hand side of equation (3) which becomes:

$$\frac{\Delta E}{E_u} = f_4\left[F_u, \frac{b}{B}, S_o, \Theta\right]. \quad (4)$$

The energy loss through the transition is equal to the difference in specific energies before and after the transition. From Fig.3, applying the specific energy equation between sections (1-1) and (3-3) yields:

$$\Delta E = E_u - E_d = \left(y_u + \frac{V_u^2}{2g}\right) - \left(y_d + \frac{V_d^2}{2g}\right) \quad (5)$$

and the relative energy loss is expressed as:

$$\frac{\Delta E}{E_u} = 1 - \frac{E_d}{E_u}. \quad (6)$$

Similarly to equation (6), from Fig.3, applying the specific energy equation between sections (1-1) and (2-2) and between sections (2-2) and (3-3) yields:

$$\frac{\Delta E_u}{E_u} = 1 - \frac{E_t}{E_u}, \text{ and} \quad (7)$$

$$\frac{\Delta E_d}{E_d} = \frac{Et}{Ed} - 1 \quad (8)$$

where;

E_u, E_t and E_d, specific energy upstream, within and downstream the water structure, respectively, ΔE= total energy loss between sections (1-1) and (3-3), ΔE_u = upstream energy loss between sections (1-1) and (2-2), ΔE_d = downstream energy loss between sections (2-2) and (3-3).By knowing either the value of velocity or water depth upstream, within and downstream the multi-vent water structure, the energy loss can be calculated by using equations (6), (7) and (8) for the known values of discharges and different contraction ratios b/B at different expansion angles Θ.

EXPERIMENTAL SET-UP AND PROCEDURE

The experiments were carried out in a rectangular open channel that is 8.0m long, 0.3m wide and 0.5m high with a glass wall (6 mm thick) and a steel plate bed. Fig.1 shows the layout of the test facility. The water is supplied from a constant head overhead tank to the flume at a desired discharge that is continuously monitored with an on-line orifice meter. The discharges were measured using a pre-calibrated orifice meter in the feeding pipeline. And in-line discharge control valve that is fitted into the main supplying pipeline was used to regulate the flow rate. Depth measurements were taken using a needle point gauge with a reading accuracy of ± 0.10 mm. The flume side walls are made up of 6 mm glass sheets. A tail gate is provided at the downstream end of the flume to maintain the required water depth of the channel flow. The water is finally collected in a sump placed in the basement from where it is pumped back to the overhead tank by a 15 Hp pump. The experiments were carried out using six different lateral contraction ratios,

b/B of 0.9, 0.8, 0.7, 0.6, 0.5 and 0.4 and five different expansion angles, Θ of 15°, 30°, 45°, 60°, 75° and 90°. Five different channel bottom positive slopes, S_o of 0.005, 0.01, 0.015, 0.02 and 0.025 were used to illustrate the effect of bottom slope on the flow characteristics due to contraction. The slopes were selected based on the flume facilities. For each combination of lateral contraction ratio, b/B, expansion angle, Θ and bottom slope, five different flow rates ranging from about 15 liters/sec to 40 liters /sec were used. The upstream water depth was adjusted to produce a Froude number ranging from 0.10 to 0.4. The flow through transition was always subcritical, but it may change to supercritical state just at the end of the transition or away from it, depending upon the incoming flow rate, the applied flume bottom slope, the expansion angle and the contraction ratio. The effect of the expansion angle Θ on the energy loss and turbulence intensities was also studied, for different lateral contraction ratios b/B and different bottom slopes S_o. Channel transitions were fabricated from transparent perspex sheets. One type of construction at the inlet was sudden and different expansions at the outlet were at expansion angles Θ of 15°, 30°, 45°, 60°, 75° and 90° downstream of two-vent water structure.

LASER DOPPLER TECHNIQUE

The experimental data were collected using the two-color back scatter Laser Doppler Velocimetry (LDV) system. Fig.2 shows a block diagram of the two-component LDV set-up used for the measurements. A 5 Watt Argon-ion laser with two laser beams; one blue (488nm) and one green (514.5nm), was focused at a measuring point from one side of the channel through an optical lens. Two Burst Spectrum Analyzers (BSA) were used to evaluate the Doppler frequencies. Subsequent computer analysis consisted of velocity bias averaging and outlier rejection. The number of samples taken at every point was 5000 bursts. This corresponds to a simple averaging time of about 100 seconds. The data rate was about (50-60) per second. Before acquiring the data, the LDV signal was checked for its quality on a 100 MHz Gold storage oscilloscope. The signal display as regular Doppler burst corresponds to a particle passing through the measuring volume. The measurements were taken at different cross-sections in the expansion zones downstream of two-vent water structure for different flow rates (Q). Fig.3 shows the location grid of the measuring stations.

With reference to the origin fixed at the channel bed and in the centre of the lower vent, as shown in Fig.3, transverse measuring volume was run to obtain the profiles of both the RMS of the streamwise and vertical turbulence intensities and streamwise and vertical mean velocity components. The measuring points were closely spaced in the region of high velocity gradient. All the measurements were made for a constant free steam water depth of 31cm irrespective of the flow rate. To obtain the vertical profiles of the mean and fluctuating flow quantities, the measurements were conducted in the vertical plane at z/b= 0 and 0.3 at different cross-sections and different flow rates. In the vertical direction at every profile, 30 measurements at 5mm intervals up to 60 mm from the bed boundary and 15mm for the rest were taken. Similarly, the measurements were conducted in the expansion zones along the centerline at relative water depth y/y_o= 0.5 to study the variation of mean and fluctuating flow characteristics.

RESULTS AND DISCUSSION

The relative total energy loss with regard to the energy upstream of the multi-vent water structure $\Delta E/E_u$ is plotted as a function of downstream expansion angles Θ of 15°, 30°, 45°, 60°, 75° and 90° at different contraction ratios b/B of 0.9, 0.8, 0.7, 0.6, 0.5 and 0.4 at various bottom slopes S_o of 0.005, 0.01, 0.015, 0.02 and 0.025, Fig.4. The total energy loss is the least value for channel contraction b/B of 0.9 and a maximum value for channel contraction b/B of 0.4. It is relatively small up to the contraction ratio b/B of 0.7. The rate of

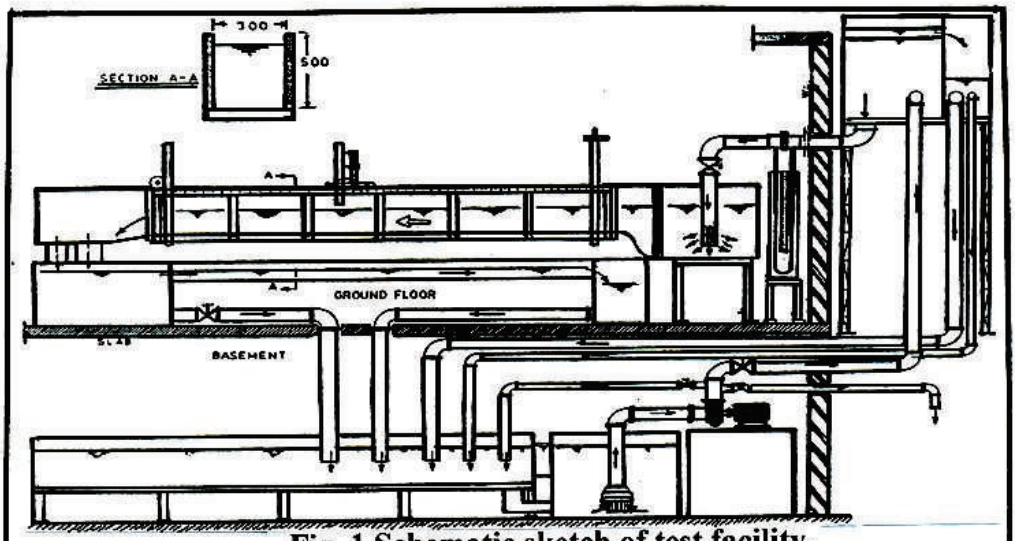

Fig. 1 Schematic sketch of test facility.

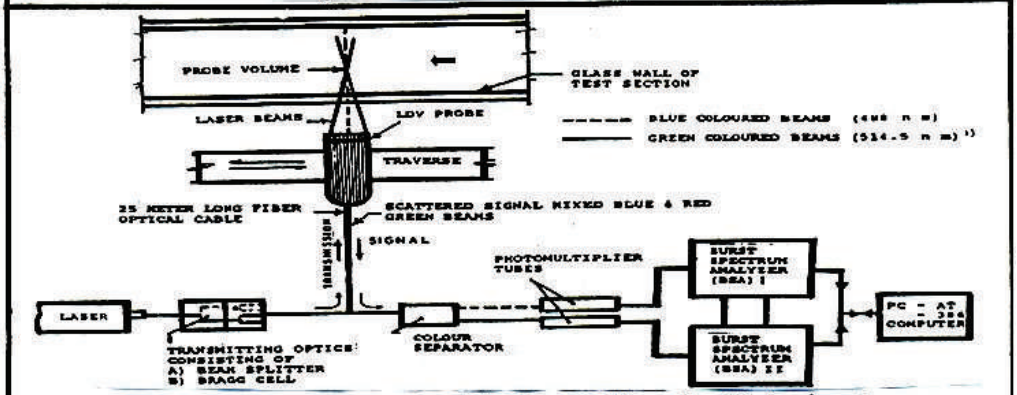

Fig. 2 Block diagram of the Laser Doppler Velocimetry.

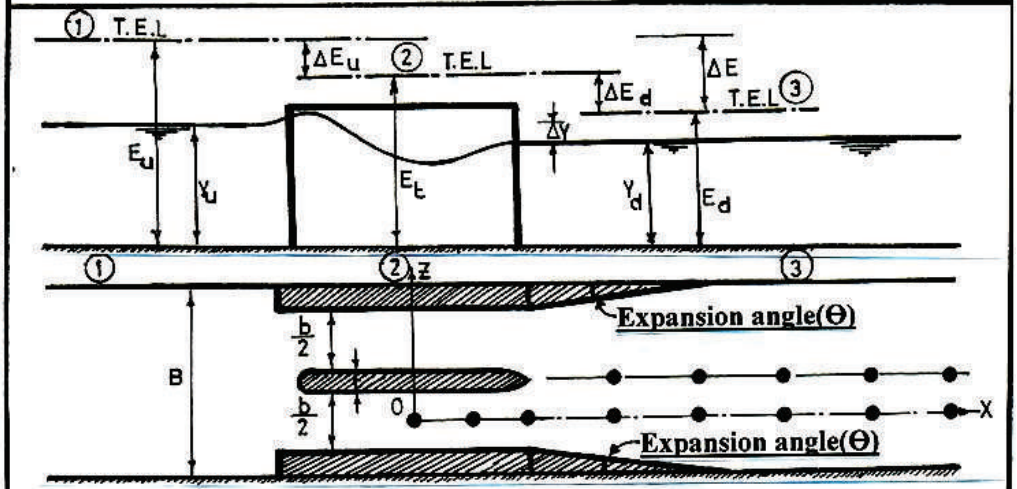

Fig. 3 Definition sketch showing the variables in the present study.

increase in energy loss, Fig.4, is almost the same between the contraction ratios b/B of 0.9 and 0.8; and of 0.8 and 0.7. By taking the value of the rate of increase in energy loss between contraction ratios b/B of 0.9 and 0.8; and of 0.8 and 0.7 as a reference, this rate of increase in energy loss has the double value between the contraction ratios b/B of 0.7 and 0.6. Similarly, this rate of increase in energy loss increases to about (5-6) times between b/B of 0.6 and 0.5 and almost about (10-12) times between contraction ratios b/B of 0.5 and 0.4 as compared to the increase in energy loss between the contraction ratios b/B of 0.9 and 0.8. This trend is almost the same for all other contraction ratios. As the expansion angle Θ increases up to 30°, the rate of increase in the head loss $\Delta E/E_u$ is relatively high for all the contraction ratios b/B, being very high for the contraction ratio b/B of 0.6. Above an expansion angle Θ of 30°, the increase in the energy loss is much slower. Particularly for expansion angles Θ greater than 45°, the energy loss is almost constant for all practical purposes. Also, as shown in Fig.4, the energy loss $\Delta E/E_u$ increases with the increase of bottom slope S_o.

Fig.5 depicts the variation of total relative energy loss $\Delta E/E_u$ with regard to the energy upstream with bottom slope S_o at different contraction ratios b/B of 0.9, 0.8, 0.7, 0.6, 0.5 and 0.4 and at different expansion angles Θ of 15°, 30°, 45° and 90°. From this figure, it can be observed that for a fixed expansion angle Θ, the trend of variation between relative energy loss $\Delta E/E_u$ and bottom slope S_o is increasing with a non-linear trend. Also, at a particular bottom slope S_o, relative energy loss $\Delta E/E_u$ decreases as the channel contraction b/B increases.

Fig.6 shows the variation of relative total energy loss $\Delta E/E_u$ with upstream Froude number F_u for different contraction ratios b/B of 0.9, 0.8, 0.7, 0.6, 0.5 and 0.4 for the flow rates Q of 15 liters/sec and 40 liters/sec. Several Froude numbers with respect to upstream depth were generated from these discharges by changing the depths for the given discharges. It can be noticed from the figure that the relationship between F_u and $\Delta E/E_u$ is a family of curves. The nature of the trend of variation of total energy loss $\Delta E/E_u$ is similar in all cases of flow. The curves are extended backward from F_u=0.05 and 0.1 for comparative purposes. With an increasing Froude number F_u, the energy loss $\Delta E/E_u$ increases with a slightly slower rate up to F_u = 0.2 say, for contraction ratios b/B > 0.5, the energy loss $\Delta E/E_u$ is small up to say F_u=0.1, after which energy loss increases rapidly as Froude number F_u increases above 0.1. The trend of variation of the relative energy loss $\Delta E/E_u$ for b/B =0.6 occupies an intermediate position between these two trends for contraction ratios b/B less than or equal to 0.7 or greater than or equal to 0.5. Again, for the same Froude number, F_u, the relative energy loss increases rapidly as the channel contraction increases. Especially, this increase is quite significant for the channel contraction greater than 0.7. For higher Froude numbers above 0.2 (in the subcritical range of flow of the present investigation), this increase is several folds compared to the minimum channel contraction b/B of 0.9.

As shown in Fig.7, for each plot, the groups of curves represent the relationship between relative upstream energy loss $\Delta E_u/E_u$ and upstream Froude number, F_u, at various contraction ratios b/B of 0.9, 0.8, 0.7, 0.6, 0.5 and 0.4 at a fixed value of angle Θ for different discharges Q of 15 liters/sec and 40 liters/sec. It clear that the trend of variation $\Delta E_u/E_u$ is quite similar in its behavioral characteristics to the one described above for total energy loss $\Delta E/E_u$, but with reduced magnitude, as ΔE_u constitutes a part of the total energy loss ΔE. The study of each plot shows that both $\Delta E_u/E_u$ and F_u increase with increasing contraction ratio b/B. The value of $\Delta E_u/E_u$ was a non-linear function of F_u. Also, it is clear that with the same value of contraction ratio b/B, the $\Delta E_u/E_u$ increases with increasing the upstream Froude number F_u. The decrease of the channel contraction reduces the separation zone, decreasing the upstream energy loss. It can be observed that by extending the lower sides of curves through the point F_u=0, $\Delta E_u/E_u$=0, the hydrostatic condition prevails. The upper limbs of the

earlier curves can be extended till reaching an optimum value of the contraction ratio b/B.

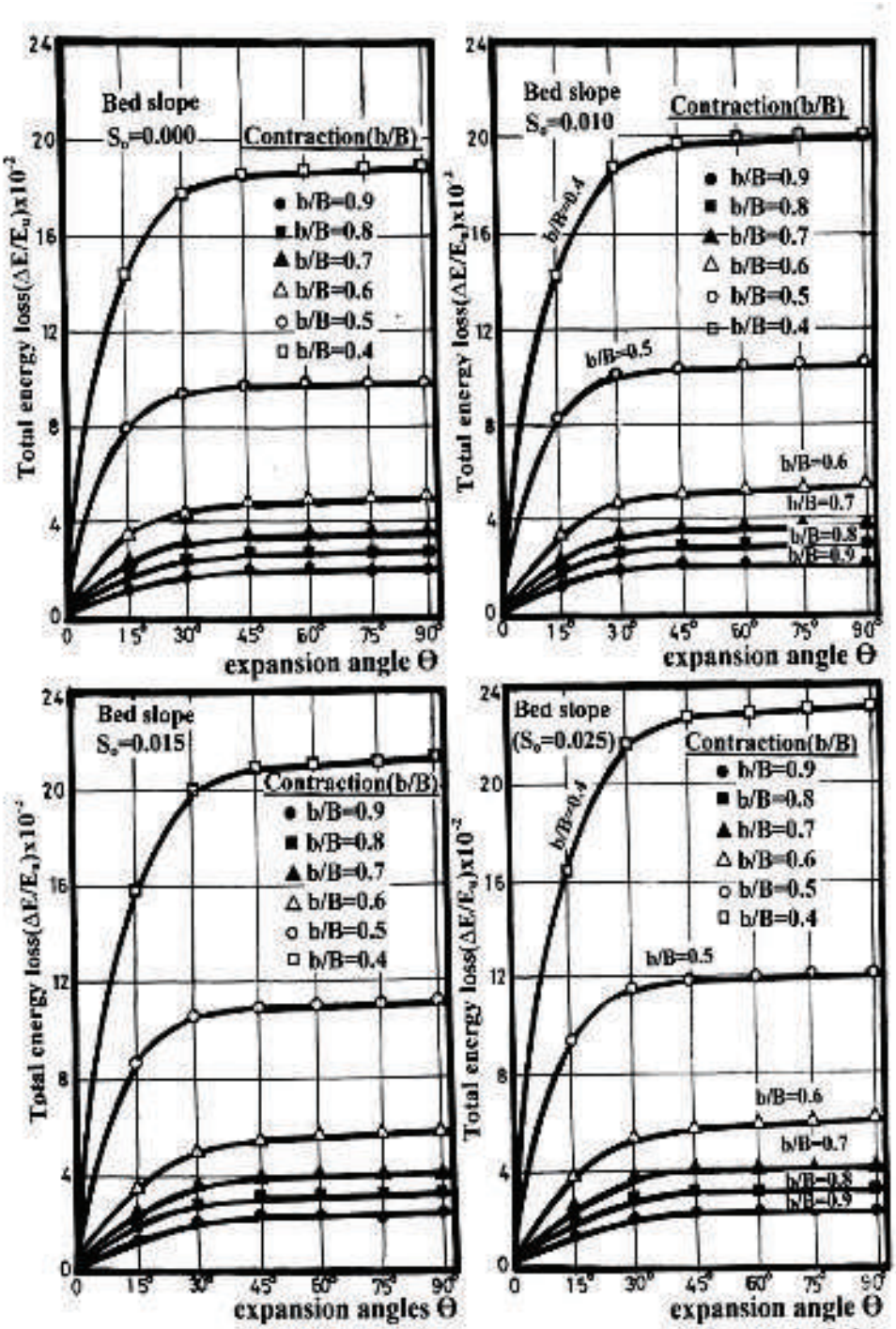

Fig.(4)Variation of total energy loss $\Delta E/E_u$ with expansion angle Θ for different contraction ratio b/B at different bottom slope S_o.

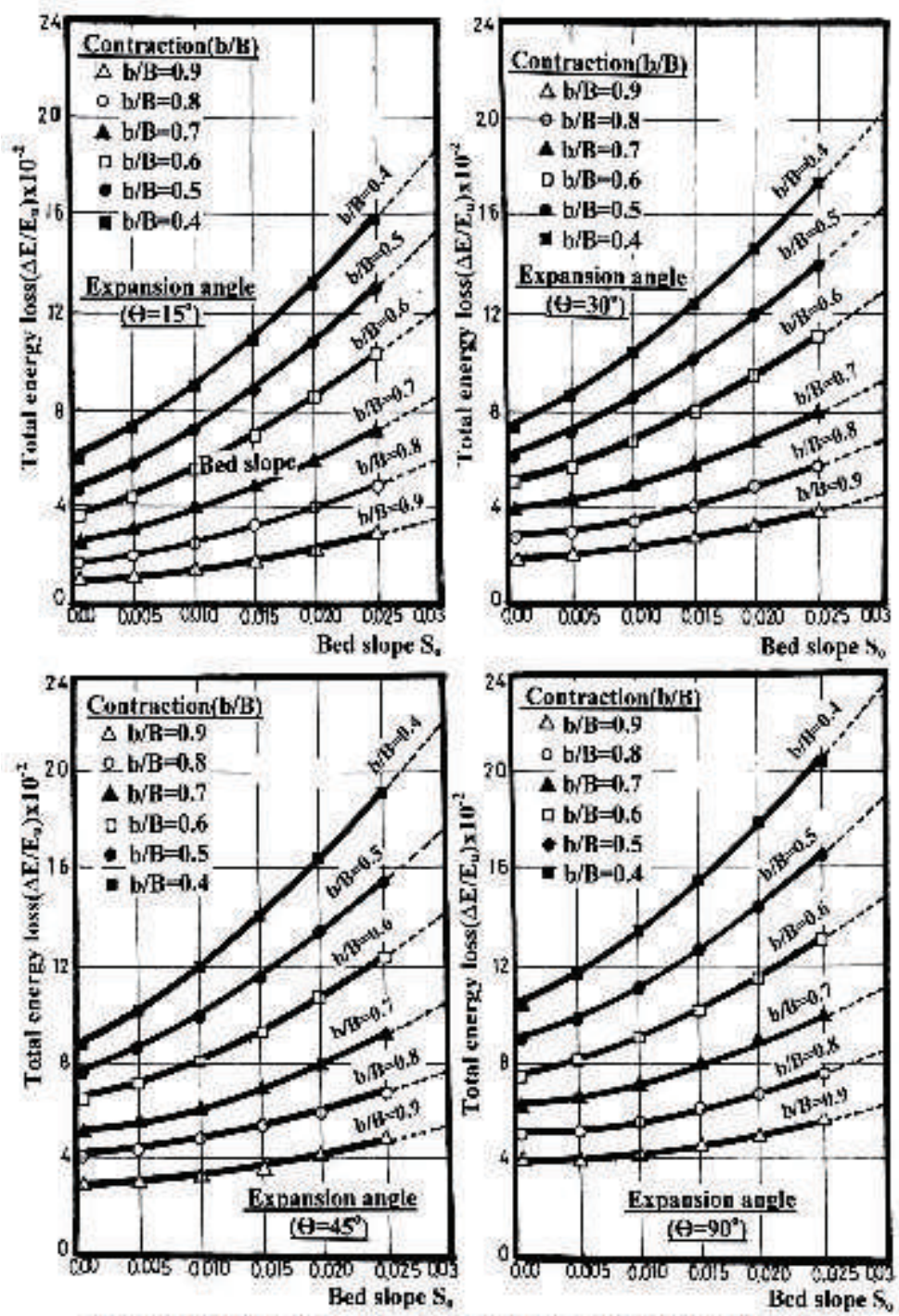

Fig.(5)Variation of total energy loss $\Delta E/E_u$ with bottom slope S_o at different contraction ratio b/B for different expansion angle Θ.

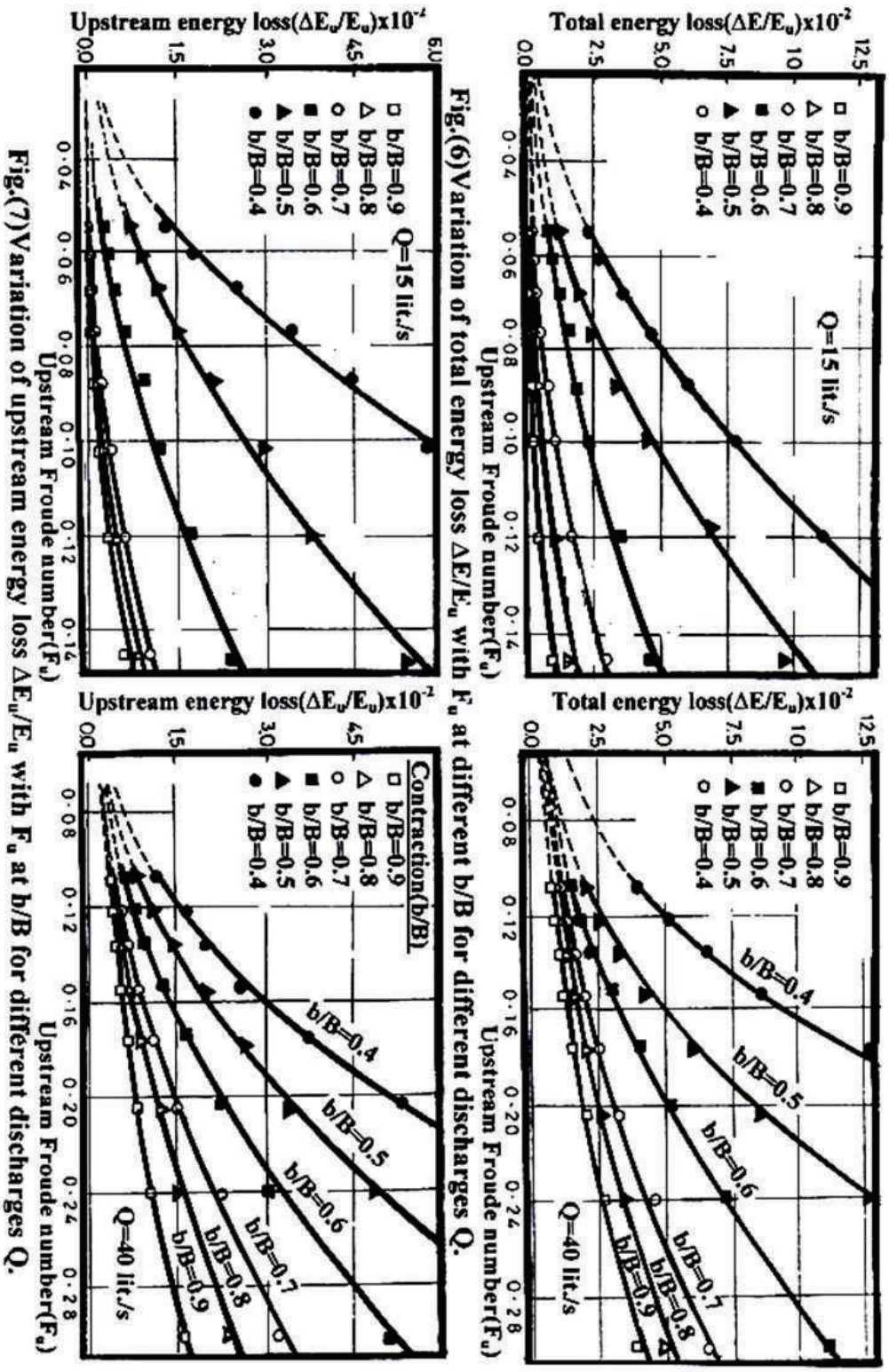

Fig.(6)Variation of total energy loss $\Delta E/E_u$ with F_u at different b/B for different discharges Q.

Fig.(7)Variation of upstream energy loss $\Delta E_u/E_u$ with F_u at b/B for different discharges Q.

Fig.8 demonstrates the relationship between relative downstream energy loss $\Delta E_d/E_d$ and upstream Froude number F_u for different contraction ratios b/B of 0.9, 0.8, 0.7, 0.6, 0.5 and 0.4 at a fixed value of expansion angle Θ for discharges of 15 liters/sec and 40 liters/sec. Again, the resulting curves indicated the same trend as discussed above for ΔE and ΔE_u. It is observed that the downstream energy loss, ΔE_d (at water structure outlet) is more than the corresponding upstream energy loss (at water structure inlet), probably due to the creation of the larger recirculating fluid mass; separated flow at the outlet of the water structure in the expansion zones. Fig.9 shows the variation in relative energy (efficiency) E_d/E_u with upstream Froude number F_u for different contraction ratios b/B of 0.9, 0.8, 0.7, 0.6, 0.5 and 0.4 for discharges of 15 liters/sec and 40 liters/sec at fixed values of expansion angle and bottom slope. From this figure, it can be observed that for discharge, the trend of variation between E_d/E_u and F_u is decreasing with a non-linear trend. Also, at a particular F_u, E_d/E_u increases as channel contraction decreases. It is observed that the effect of F_u on E_d/E_u is significant. E_d/E_u increases non-linearly with the decrease of F_u. Also, E_d/E_u increases as the discharge decreases. Fig.10 shows the variation of the relation of water depth Y_d/Y_u as a function of upstream Froude number F_u at different contraction ratios b/B of 0.9, 0.8, 0.7, 0.6, 0.5 and 0.4 for discharges of 15 liters/sec and 40 liters/sec at fixed values of bottom slope and expansion angle. It is clear that the trend of variation Y_d/Y_u is quite similar in its behavioral characteristics to the one described above for relative energy E_d/E_u. The study of each plot shows that Y_d/Y_u increases as F_u decreases with the decrease of channel contraction. The value of Y_d/Y_u was a non-linear function of F_u. Fig.11 depicts the variation of relative heading up $\Delta Y/Y_u$ as a function of upstream Froude number F_u for different contraction ratios b/B of 0.9, 0.8, 0.7, 0.6, 0.5 and 0.4 for discharges of 15 liters/sec and 40 liters/sec at fixed values of expansion angle Θ and bottom slope S_o. From this figure, it is observed that the effect of F_u on Y_d/Y_u is significant. Y_d/Y_u increases non-linearly with the increase of F_u. Also, at a fixed discharge Q, the trend of variation between Y_d/Y_u and F_u is increasing with a non-linear trend. Also, at a particular F_u, Y_d/Y_u increases as the channel contraction increases.

Figs.12 and 13 depict the variation of streamwise and vertical components of turbulence intensities $ú/U_o$ and $ü/U_o$ as functions of channel depth y/y_o in the expansion zone of water structure at different expansion angles Θ of 15°, 30°, 45° and 90° and at different contraction ratios b/B of 0.7 and 0.5 for a discharge of 40 liters/sec along the depth at different cross-sections. The trends of variation of $ú/U_o$ and $ü/U_o$ are similar in all the cases of expansion angles. The trends of $ú/U_o$ and $ü/U_o$ in the expansion zones in all the cases of expansion angles Θ show to have higher values close to the bed, following a gradual fall in the wall region defined by $y/y_o<0.2$, reaching minima in the core region defined by $0.2<y/y_o<0.6$. Turbulence intensities $ú/U_o$ and $ü/U_o$ rise gradually and then rapidly in the upper region (free surface region) defined by $y/y_o>0.6$, reaching the maximum at the free surface. The minimum turbulence intensities $ú/U_o$ and $ü/U_o$ always lie in the core region. The maximum turbulence intensities occur close to the bed or at the free surface depending on the location of the profile station. The nature of these variations is similar in all the cases of expansion angles, contraction ratios and discharges. Fig.13 shows the turbulence intensities $ú/U_o$ and $ü/U_o$ at b/B = 0.5 and the expansion angles Θ of 15°, 30º, 45° and 90°. The profiles of $ú/U_o$ and $ü/U_o$ in the expansion zones of the hydraulic structures, which depict the turbulence behavior more dearly, at an expansion angle Θ of 90°, indicate large magnitudes of turbulence in the wall and free surface regions, with fairly uniform turbulence in the core region. However, for an expansion angle of Θ=15°, the turbulence profile is fairly uniform with comparatively less increase of the turbulence in wall and free surface regions. In case of an expansion angle of Θ=90°, as shown in Fig.13, the nature of variation in turbulence intensities $ú/U_o$ and $ü/U_o$ at the entry of expansion zones and subsequent sections downstream is somewhat distinct

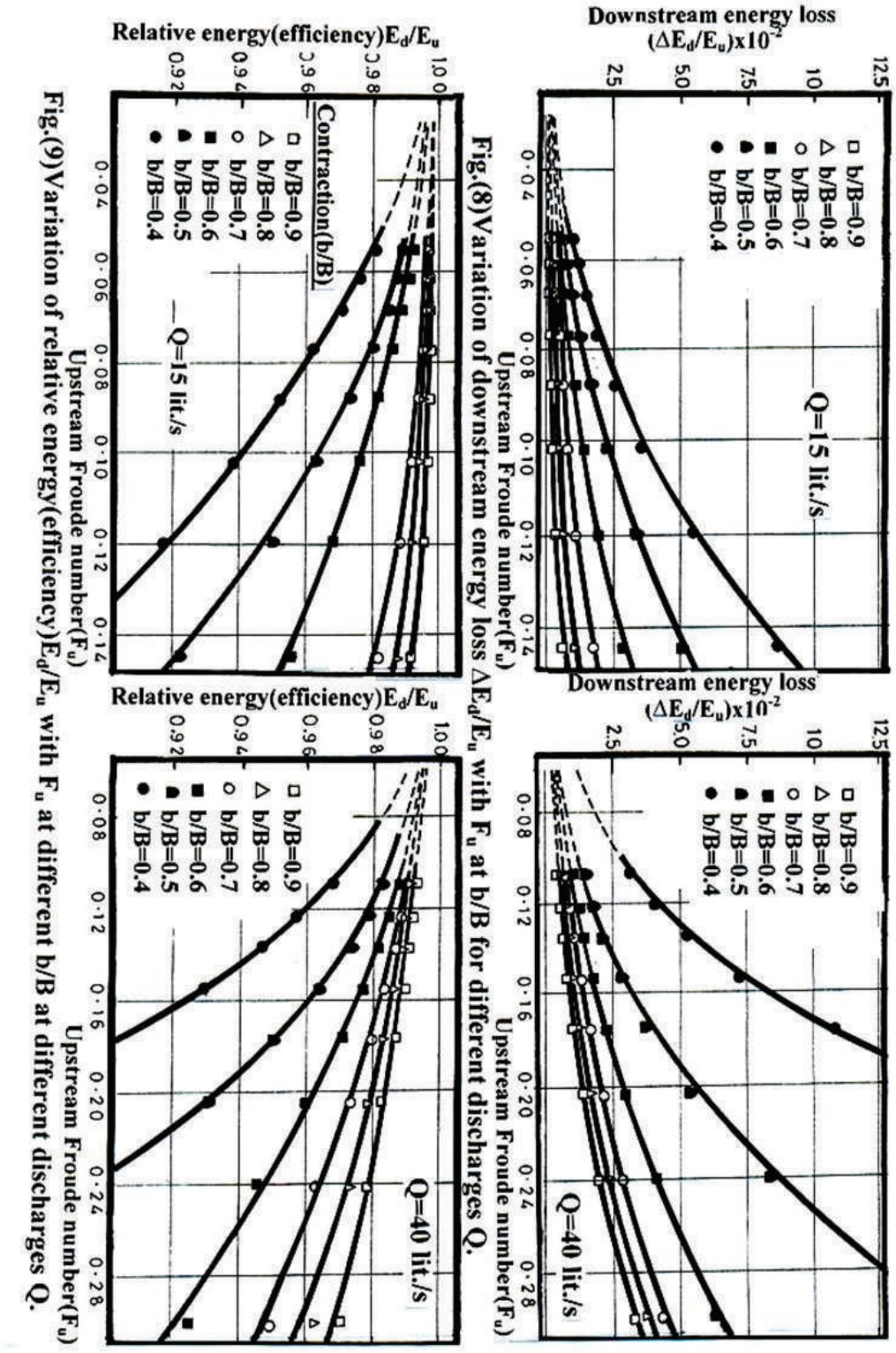

Fig.(8)Variation of downstream energy loss $\Delta E_d/E_u$ with F_u at b/B for different discharges Q.

Fig.(9)Variation of relative energy(efficiency)E_d/E_u with F_u at different b/B at different discharges Q.

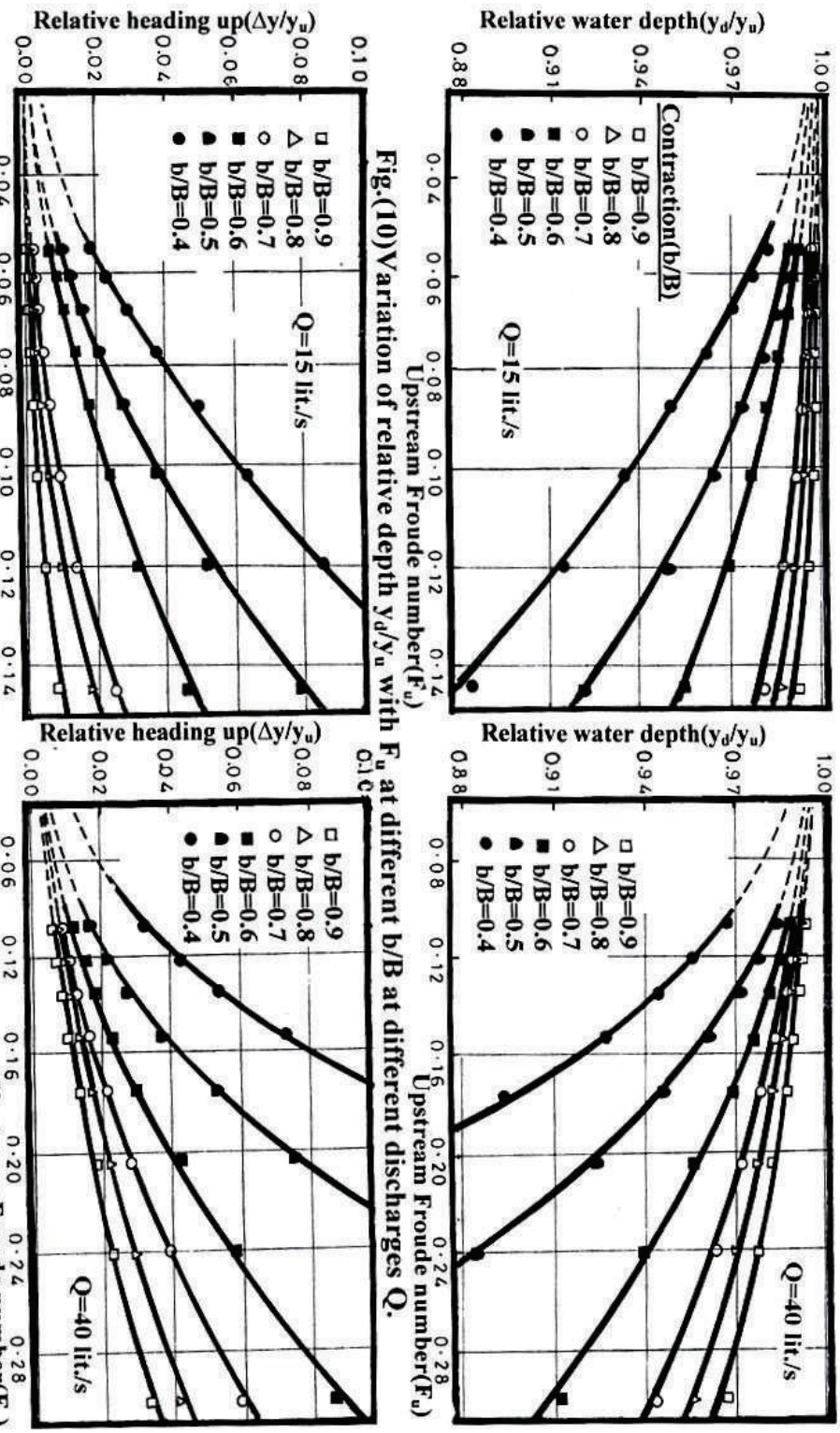

Fig.(10)Variation of relative depth y_d/y_u with F_u at different b/B at different discharges Q.

Fig.(11)Variation of relative heading up $\Delta y/y_u$ with F_u at different b/B at different discharges Q.

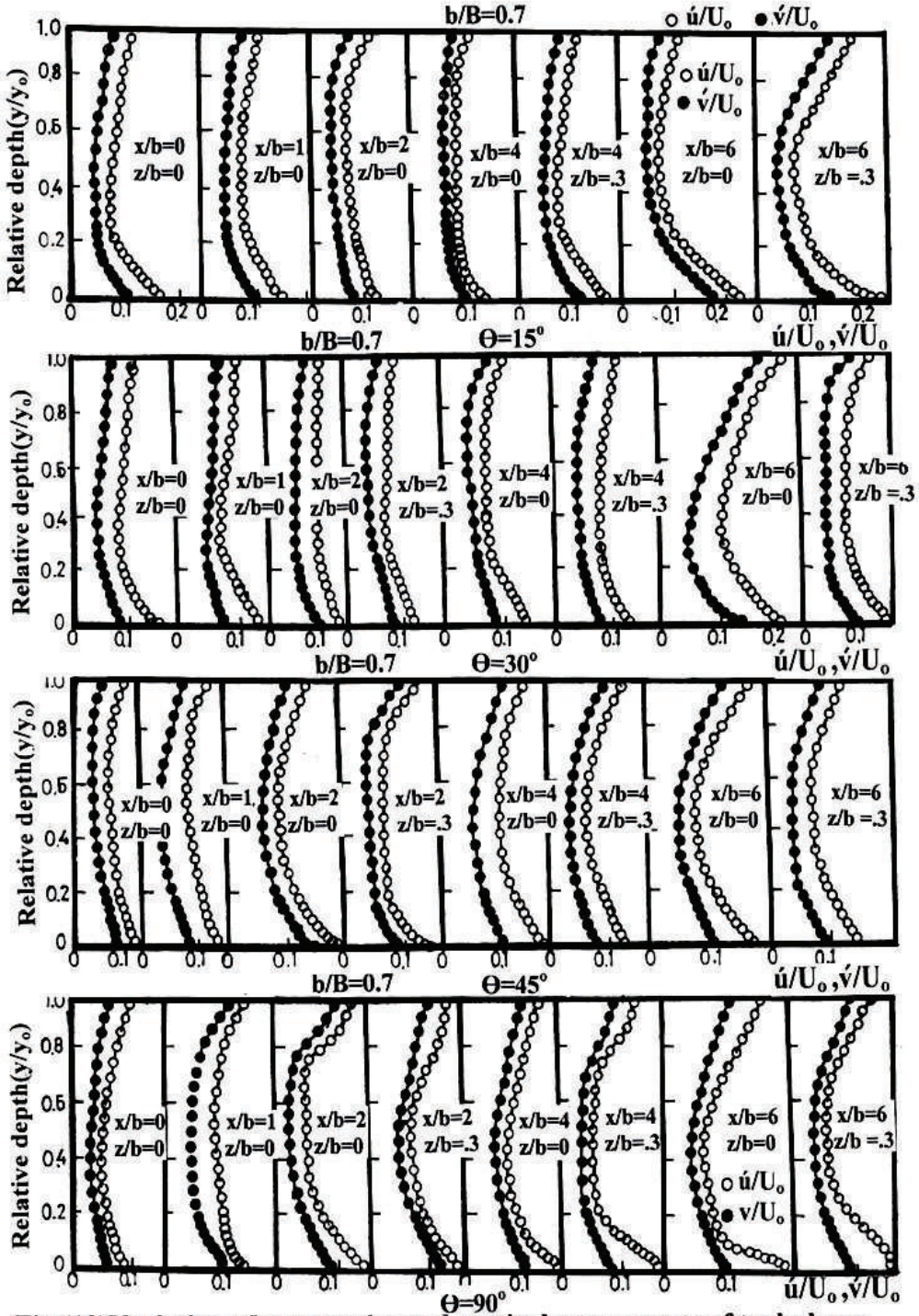

Fig.(12)Variation of streamwise and vertical components of turbulence intensities ú/U_0 and v́/U_0 with y/y_0 in the expansion zones at b/B=0.7 at expansion angles Θ=15°, 30°,45° and90°for Q=30 lit./s .

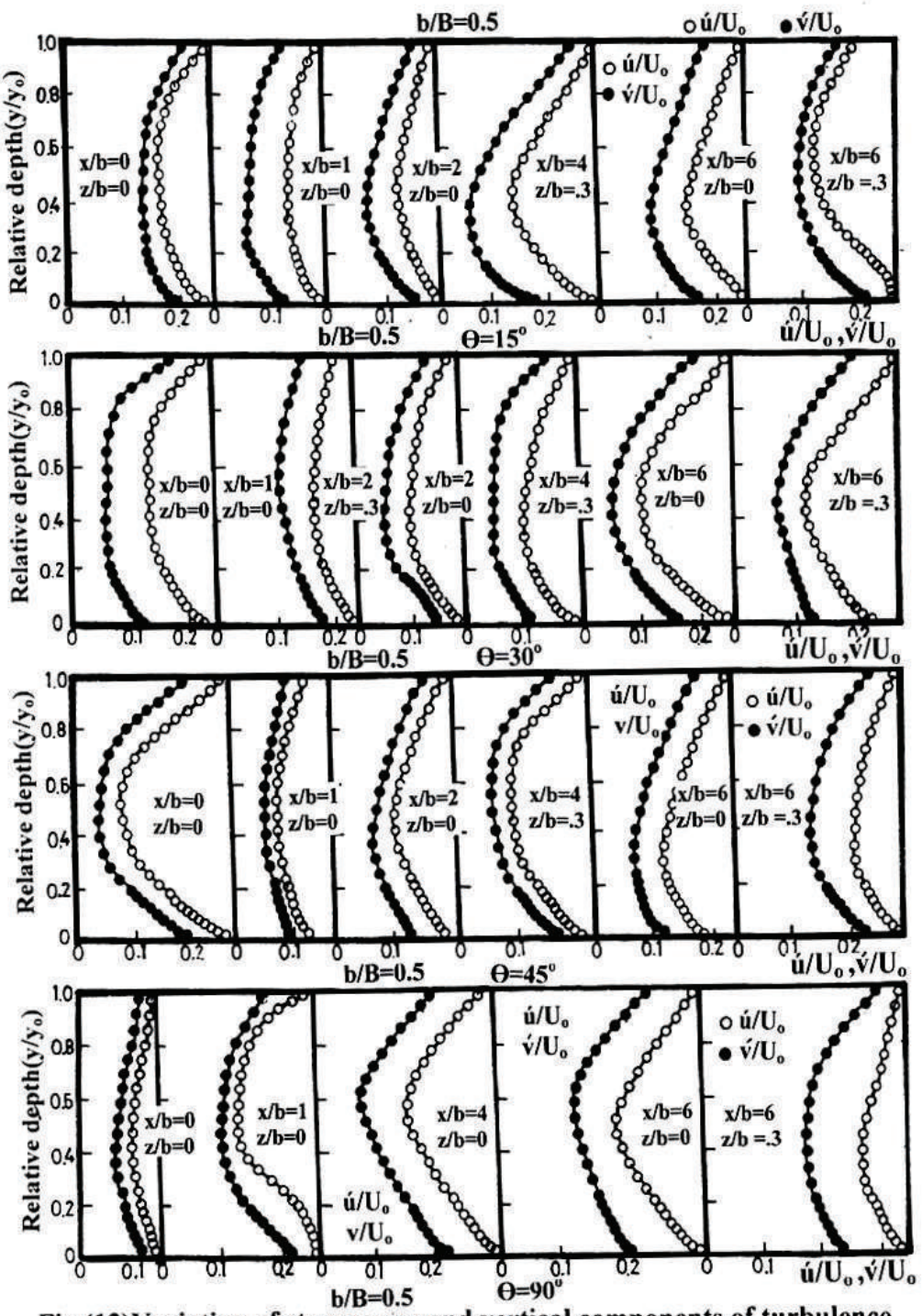

Fig.(13)Variation of streamwise and vertical components of turbulence intensities $\acute{u}/U_o$ and v/U_o with y/y_o in the expansion zones at b/B=0.5 at expansion angles $\Theta=15^o, 30^o, 45^o$ and 90^o for Q=30 lit./s .

compared to the turbulence profiles in the case of gradual expansion Θ=15°. Herein, in the core region of sudden expansion Θ of 90°, turbulence intensity profiles ú/U_o and ύ/U_o do not exhibit the tendency towards constancy unlike in the gradual expansion, Θ=15°. Generally, in sudden expansion Θ=90° after reaching the minimum turbulence intensities ú/U_o and ύ/U_o as the flow distance increases from the wall, the turbulence tends to increase consistently till the free surface is reached. Turbulence intensities are particularly largest ú/U_o = 45%, ύ/U_o = 29% and ú/U_o =55%, ύ/U_o=35% at x/b=2, z/b=0 and x/b=2, z/b=0.3 closer to the wall region and free surface region, respectively. Similarly, both the turbulence intensities ú/U_o and ύ/U_o are large at all the sections investigated downstream of the inlet of expansion zone in 90° sudden expansion in the wall region and free surface region. The general trend in the variation of depthwise turbulence observed in this work is similar in the expansion zone up to x/b=6. Generally, the turbulence intensities ú/U_o and ύ/U_o grow rapidly after the flow separation and spread in the vertical direction in all cases of expansion angle. Also, it can be seen that gradual expansion (Θ of 15°) is more effective in minimizing the turbulence intensity in the expansion zones compared to the 90° expansion angle. Downstream of the inlet of the expansion zone along the centerline, it is noted that farthest downstream at x/b=6, turbulence intensities ú/U_o and ύ/U_o along the axis and z/b=0.3 are lowest for 15° expansion. However, they exhibit a sharp increase at the free surface. Concluding, gradual expansion decreases the depthwise turbulence intensities ú/U_o and ύ/U_o in wall and free surface regions compared to sudden expansion. This dampening effect could be attributed to the reduced magnitude of surface waves observed in the gradual expansion compared to relatively larger surface waves in the 90° sudden expansion. Further, the results show the influence of the expansion angle (diversion angle) on the turbulence intensities ú/U_o and ύ/U_o, which decrease with reduced diversion angle. Moreover, with the increasing expansion and channel contraction, the vertical variation in turbulence intensities ú/U_o and ύ /U_o becomes more pronounced, changing rapidly in the wall, core and the free surface regions.

Figs.14 and 15 depict the variation of streamwise and vertical components of turbulence intensity fluctuations ú/U_o and ύ/U_o along the centerline at a relative water depth y/y_o = 0.5 above the bed in the expansion zones for the flow of 40 liters/sec, at different contraction ratios b/B of 0.5 and 0.7, at different expansion angles Θ of 15°, 30° and 90°. Clearly, the trend of variation in turbulence intensities ú/U_o and ύ/U_o is quite similar in all the cases of expansion angle Θ and contraction ratio b/B. Following a slight general fall, reaching a minimum, turbulence rises rapidly to reach a maximum with a subsequent monotonous decrease along the distance away from the outlet of the hydraulic structure. Generally, maximum turbulence intensities ú/U_o and ύ/U_o occur at the same location with slight shift noticed for gradual expansion Θ=30°. The salient features of the variation observed are as follows. For contraction ratios b/B of 0.7 and 0.5, the minimum values of ú/U_o and ύ/U_o occur at 0< x/b<1.5 for all the expansion angles. The maximum values of ú/U_o and ύ/U_o occur at 2.2<x/b< 4.5. Similar trends are observed for turbulence intensities ú/U_o and ύ/U_o for all contraction ratios b/B of 0.5 and 0.7 at the different expansion angles Θ of 15°, 30° and 90°. It may be concluded that downstream of the water structures beyond specific values of x/b, for instance 3.8, turbulence intensities ú/U_o and ύ/U_o are always higher in the case of 90° sudden expansion and lower for most gradual expansion of 15°, for all contraction ratios b/B of 0.7 and 0.5. The trend is exactly opposite as observed for x/b< 2.7. Also, it may be concluded that turbulence intensity beyond x/b = 4.1 from the centre of the hydraulic structure decreases with decreasing the angle of diversion, being subsequently higher as for sudden expansion Θ=90°, the lowest for gradual expansion Θ of 15° and intermediate for gradual expansion of Θ=30°. The trend is reversed for x/b < 2.7, where the turbulence intensity is higher for

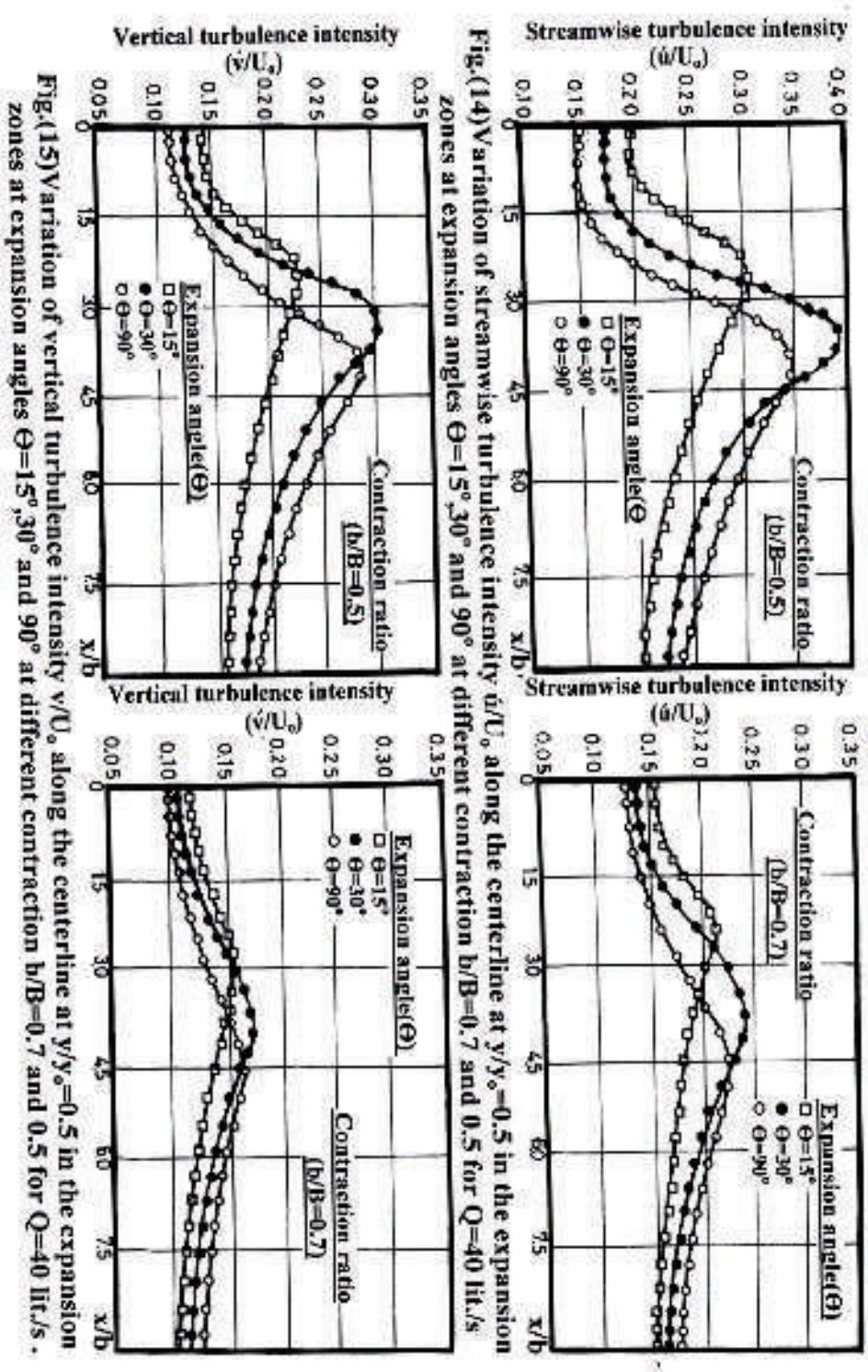

Fig.(14)Variation of streamwise turbulence intensity u/U_o along the centerline at y/y_o=0.5 in the expansion zones at expansion angles Θ=15°,30° and 90° at different contraction b/B=0.7 and 0.5 for Q=40 lit./s

Fig.(15)Variation of vertical turbulence intensity v/U_o along the centerline at y/y_o=0.5 in the expansion zones at expansion angles Θ=15°,30° and 90° at different contraction b/B=0.7 and 0.5 for Q=40 lit./s .

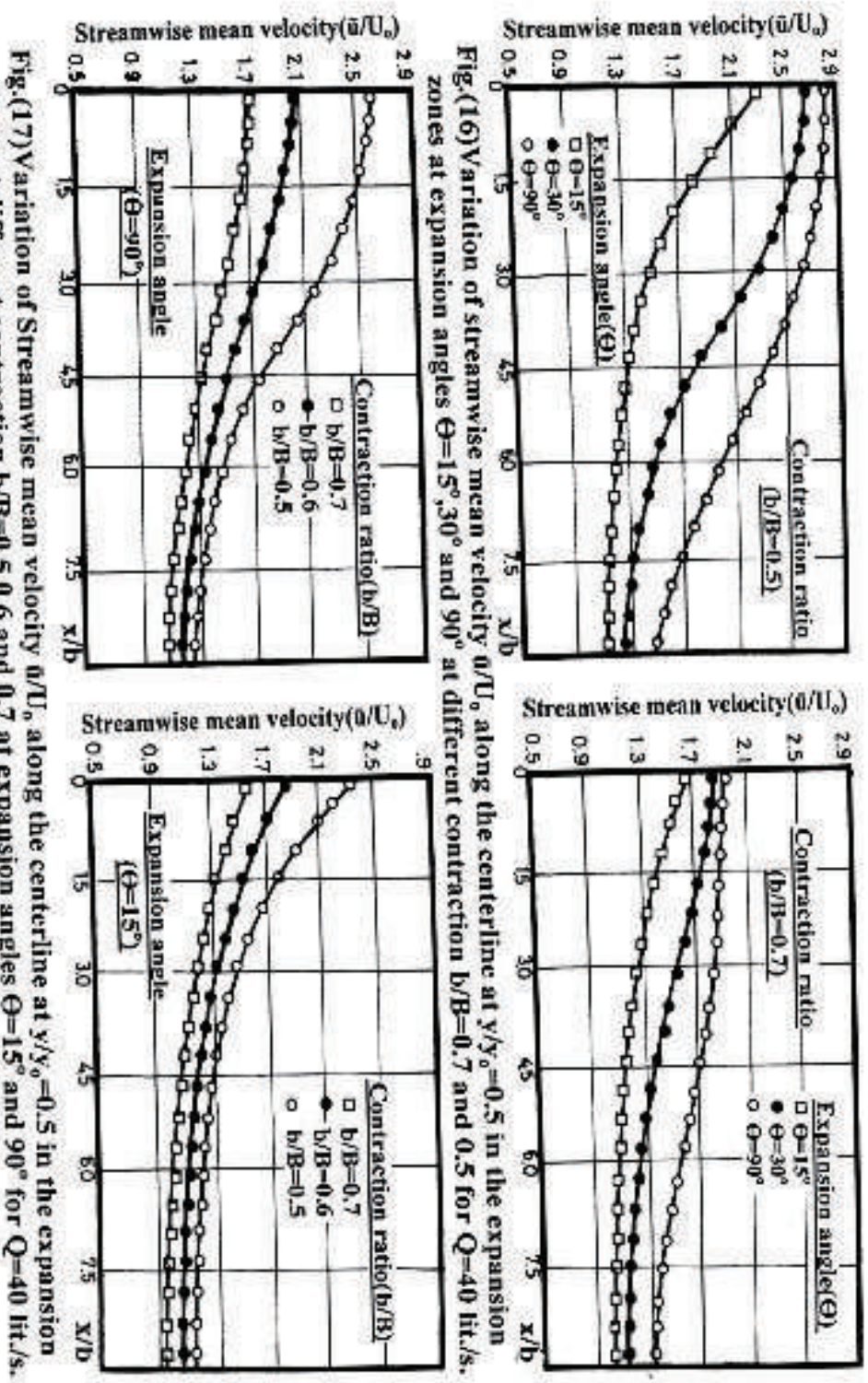

Fig.(16)Variation of streamwise mean velocity u/U_o along the centerline at y/y_o=0.5 in the expansion zones at expansion angles Θ=15°,30° and 90° at different contraction b/B=0.7 and 0.5 for Q=40 lit./s.

Fig.(17)Variation of Streamwise mean velocity u/U_o along the centerline at y/y_o=0.5 in the expansion zones at different contraction b/B=0.5,0.6 and 0.7 at expansion angles Θ=15° and 90° for Q=40 lit./s.

gradual expansion Θ=15° and lower for 90° sudden expansion. At x/b of 2.7 up to 4.2, the maximum turbulence intensities ú/U_o and ǘ/U_o occur for all the expansion angles at different contraction ratios b/B and all different spanwise locations. Also, with increasing channel contraction, the turbulence intensities ú/U_o and ǘ/U_o increase for all the cases.

CONCLUSIONS

The conclusions arising out from this study can be summarized as follows:

Form the evidence of the variation of the total energy loss $\Delta E/E_u$ with the expansion angle in the expansion zones downstream of the water structures, it appears that up to an expansion angle of 30°, decreasing the expansion angle, the head loss decreases, but above this expansion angle of 30°, the effect of the boundary is insignificant. The energy loss is quite high if the contraction ratio b/B > 0.7. The energy loss increases rapidly up to an expansion angle of 30° and tends to remain constant above an expansion angle of 45°. Thus, an expansion angle of 30° appears to be a critical angle defining a border value between the maximum energy loss and the value up to which total energy loss increases rapidly as the expansion angle increases form 0° to 30°. The results indicate that the most significant differences in energy loss occur with an expansion angle in the range less than 45°. The total energy loss $\Delta E/E_u$, upstream energy loss $\Delta E_u/E_u$ and downstream energy loss $\Delta E_d/E_d$ of multi-vent water structures, increase with increasing the value of both upstream Froude number and channel contraction. The downstream energy loss (at hydraulic structure outlet) is more than the corresponding upstream energy loss (at hydraulic structure inlet), probably due to the creation of the large recirculating fluid mass, separated flow at outlet of the hydraulic structure in the expansion zones.

The streamwise turbulence intensities ú/U_o and ǘ/U_o are higher nearer the bed in the wall region defined by $y/y_o \leq 0.2$ due to wall effect and the free surface region defined by $y/y_o > 0.6$ due to free surface effect. In the intermediate core region defined by $0.2 < y/y_o \leq 0.6$, minimum turbulence intensities ú/U_o and ǘ/U_o occur, and consistently correspond to the maximum streamwise mean velocity ū/U_o, occurring in the same zone approximately at the same location with the local velocity gradient being zero. In the expansion zones, gradual expansion decreases the turbulence intensities ú/U_o and ǘ/U_o in wall and free surface regions compared to sudden expansion. The maximum values of turbulence intensities ú/U_o and ǘ/U_o occur either close to the bed or at the free surface. As a comprehensive observation, it is noted that the streamwise turbulence ú/U_o is always greater compared to the vertical turbulence ǘ/U_o. Also, it is concluded that with decreasing the expansion angle and channel contraction in the expansion zone, turbulence intensities ú/U_o and ǘ/U_o decrease in all cases. Along the depth, the trend of variation of turbulence intensities is similar at all expansion angles in the expansion zones of hydraulic structures; these increase or decrease simultaneously in all cases of expansion angle.

NOMECLATURE

b Width of hydraulic structure (total width).
B Natural channel width.
ū Streamwise mean velocity in x-direction.
U_o Streamwise mean free stream velocity. averaged over the cross-section.
ù Streamwise component of turbulence intensity in x- direction (RMS).
v̄ Vertical mean velocity in y-direction.
ǘ Vertical component of turbulence intensity in y-direction (RMS).
x Longitudinal axis along channel length.
y Transverse axis along channel height.
z Transverse axis along channel width.
S_o Bottom slope.
Q Flow discharge**.**

S_o Bed slope.

Θ Expansion angle.

RMS Root Mean Square.

REFERENCES

Amino, R.S. and Goel, P. 1985. Computations of Turbulent Flow Beyond Backward Facing Steps Using Reynolds Stress Closure, *AIAA J.,* 23 (23): 1356-1361.

Chow, V.T. 1959. Open Channel Hydraulics, Mc-Graw Hill Book Co., New York, 461-468.

Etheridge, D.W. and Kemp, P.H. 1978. Measurements of Turbulent Flow Downstream of a Rearward Facing Step, *Fluid Mech.,* (3).

Formica, G. 1955. Preliminary Test on Head Losser in Channels Due to Cross-Sectional Changes, *L. Energia Electrica,* Milano, 32 (7): 554-568.

Garde, R.J. 1994. Turbulent Flow, Published by H.S. Poplai for Wiley Eastern, Limited, New Age International Limited, 4835/24, Ansari Road, Daryaganj, New Delhi-110002.

Grade, H. 1993. The Turbulent Flow Models in Open Channel Flows, Monograp, A.S. Balkema Puplishers, New Road, V.T 08079, New Delhi, India.

Guoren, D. and Xiaonan, T. 1992. Some Measurements of a Turbulent Structure in an Open Channel, Proceedings of the Conference of Flow Modelling and Turbulence Measurements, Ed., Zaiobao, Hemisphere Publishing Corporation, Washington.

Nakagawa, H. and Nezu, I. 1995. Experimental Investigation on Turbulent Structure of Backward Facing Step Flow in an Open Channel. *J. of Hydr. Research*, 25 (1).

Nakagawa, H. and Nezu, I. 1987. Experimental Investigation on a Turbulent Structure of Back Facing Step Flow in an Open Channel. *J. Hydraulic Research*, IAHR, 25: 67-88.

Nezu, I. and Rodi, W. 1986. Open Channel Flow Measurements with Laser Doppler Velocimetry, *J. Hydraulic Engg. ASCE*, 112: 335-355.

Nezu, I. and Nakagawa, H. 1993. Turbulence in Open Channel Flow, IAHA-Monograph, A.A. Balkma Publishers, Old Post Road, Brookfield, VTO 5035, USA.

Rodi, W. 1993. Turbulence Models and their Application in Hydraulics, IAHR Monograph, A.A. Balkema Publishers, Old Post Road, Brookfield, VTO 5036, USA.

Song, T. and Chinew, Y. 2001. Turbulence Measurement in Nonuniform Open Channel Flow Using Acoustic Doppler Velocimeter (ADV). *J. Engg. Mech.,* 127 (3): 219-231.

Sukhodolov, A. and Thiele, M. 1998. Turbulence Structure in a River Reach with Sand Beds, *Water Resour*., 34 (5): 1317-1334.